

# Frequency-Modulated Continuous-Wave Laser Ranging With Sub-Nyquist Sampling Rate Using Asymmetric Chirped Waveforms

Bowen Qiu<sup>1</sup>, Gang Hu<sup>1</sup>, Zhongyang Xu<sup>1\*</sup>, Xingbang Zhu<sup>1,2</sup>, Yamei Zhang<sup>1\*</sup>,  
and Shilong Pan<sup>1\*\*</sup>

<sup>1</sup>Key Laboratory of Radar Imaging and Microwave Photonics, Ministry of Education, Nanjing University of Aeronautics and Astronautics, Nanjing 210016, China

<sup>2</sup>The 41st Institute of CETC, Qingdao 266555, China

\*Member, IEEE

\*\*Senior Member, IEEE

Manuscript received 21 September 2022; accepted 4 October 2022. Date of publication 10 October 2022; date of current version 28 October 2022.

**Abstract**—We propose a frequency-modulated continuous-wave (FMCW) laser range with sub-Nyquist sampling rates in which asymmetric chirped waveforms are used. Different de-chirped signals can be generated since the up-chirp and the down-chirp sections have different chirp rates. The distances are extracted at a sub-Nyquist sampling rate using a modified Vernier sampling, in which the sub-Nyquist sampling technique ratio is reconfigurable by changing the ratios of the chirp rates. A demonstrated experiment is carried out. The lengths of fiber can be measured with a sub-Nyquist sampling ratio of 1/10. Therefore, the proposed method reduces the sampling rate in the FMCW laser ranging system using Vernier sampling. Moreover, only a single-shot sampling is required, which reduces the complexity of the Vernier sampling.

**Index Terms**—Sensor phenomena, laser ranging sensors, frequency-modulated continuous-wave (FMCW), sub-nyquist sampling, vernier sampling.

## I. INTRODUCTION

Laser ranging has great potential in 3-D imaging [1], [2], [3], autonomous driving [4], [5], [6], natural disaster monitoring [7], [8], etc. Compared with pulsed time-of-flight (ToF) laser ranging [9], [10], frequency-modulated continuous-wave (FMCW) laser ranging has the advantages of low peak power and anti-interference [11], [12], [13]. Meanwhile, millimeter-level precision can be achieved at a distance of kilometers in FMCW laser ranging [14]. The FMCW method relies on chirped waveforms whose frequency linearly changes with time. The local and received signals beat with each other in a photodetector to obtain de-chirped signals, whose frequencies are proportional to the distances of targets. Then, a Fourier transform for the sampled de-chirped signal is implemented to obtain the frequencies, which requires a sampling rate much higher than the ToF laser ranging. According to Nyquist sampling theory, the sampling rate should be more than twice as high as the de-chirped frequencies to ensure the reconstruction of the de-chirped signals [15]. The higher sampling rate indicates more sampling points, which generates massive data and requires a large storage capacity compared to the ToF laser ranging.

To reduce the sampling rate and data volume, sub-Nyquist sampling methods are proposed, in which compressed sampling is one of the widely used methods [16], [17]. In compressed sampling, the signal is first sampled using a specific nonuniform sparse sampling matrix [17]. The second step is to recover the original signal from the sparse signal with algorithms. However, the implementation of nonuniform sampling requires additional devices [18]. Moreover, the complex recovery algorithms limit the data processing speed, which may reduce the measurement rate.

Vernier sampling is also a kind of sub-Nyquist sampling method, which has been widely used in interferometric fiber sensors, dual-comb spectroscopy, and dual-comb ranging [19], [20], [21], [22]. Using a principle similar to that of a Vernier caliper, the signals are usually sampled at different rates in the Vernier sampling process. The distance can be recovered with an algorithm much simpler than compressed sampling. For example, optical Vernier sampling has been used to solve distance aliasing, in which a dual-comb-swept laser is used to sample the optical interferometry signals [21]. However, in the Vernier sampling process, two sampling devices must be applied to solve the distance aliasing. To further reduce the sampling rates, more parallel sampling processes must be implemented [22], which largely enhances the cost of the system. In [21], although a single-shot sampling is achieved, it is the two parallel sampling processes that are achieved by two combs with different free spectral ranges (FSRs) so that a larger absolute distance can be recovered. Moreover, since the sampling rates of the devices are usually fixed, the sub-Nyquist sampling ratio of the system is not reconfigurable.

In this letter, we achieve FMCW laser ranging with a sub-Nyquist sampling rate based on a modified Vernier sampling. An asymmetric chirped waveform is employed in the FMCW ranging system so that the up-chirp and down-chirp sections generate different de-chirped signals due to the different chirped rates. As a result, two aliasing frequencies can be simultaneously obtained using a single-shot sampling technique with a sub-Nyquist sampling rate. Then, the frequencies of the two de-chirped signals are recovered based on the Vernier sampling principle, which is finally used to calculate the distance. A demonstrated experiment is carried out in which the bandwidth of the chirped waveform is 6 GHz. The durations of the up-chirp and down-chirp sections are 1 and 1.2  $\mu$ s, respectively. The de-chirped signal is sampled at a rate less than 1/6 of the Nyquist sampling rate. The sampling rate can be further reconfigured to less than 1/10 of

Corresponding author: Zhongyang Xu (e-mail: xzy@nuaa.edu.cn).

Associate Editor: X. Shu.

Digital Object Identifier 10.1109/LENS.2022.3212790

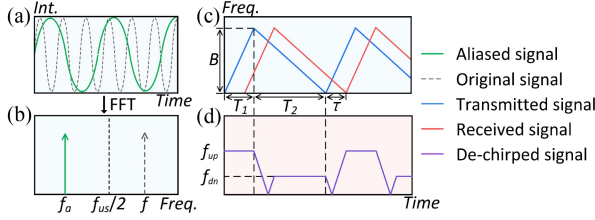


Fig. 1. (a) and (b) Frequency aliasing due to sub-Nyquist sampling. (c) and (d) FMCW laser ranging using asymmetric chirped waveforms.

the Nyquist sampling rate by simply changing the chirp rates. The length of optical fiber can be measured with an accuracy of less than 6.1 cm.

## II. PRINCIPLE AND SYSTEM

In FMCW laser ranging, the distance of a target is calculated from the frequency of the de-chirped signal as

$$R = \frac{cTf_b}{B} \quad (1)$$

where  $f_b$  is the frequency of the de-chirped signal,  $c$  is the speed of light in vacuum, and  $T$  and  $B$  are the duration and the bandwidth of the chirped signal, respectively. The frequency of the de-chirped signal can be extracted using a discrete Fourier transform (DFT). Fig. 1(a) and (b) show the sub-Nyquist sampling of a single-tone signal. The relationship between the actual frequency  $f$  and the aliased frequency  $f_a$  can be given by

$$f = n f_{us} \pm f_a \quad (2)$$

where  $f_{us}$  is the sampling rate,  $n$  is an integer, and  $f_a$  is less than half of the sampling rate ( $f_{us}/2$ ). Obviously, the actual frequency cannot be recovered using only one sampling rate since the value of  $n$  is not determined. To solve the frequency aliasing, Vernier sampling can be used [20], in which two sub-Nyquist samplings at different rates are always required. Then, the actual frequency can be recovered based on a principle similar to the Vernier caliper, from which the distance of the target can be calculated.

Here, we propose a modified Vernier sampling method for the FMCW laser range, in which only a single-shot sub-Nyquist sampling process is required. An asymmetric chirped waveform is used to modulate the lightwave. The bandwidths of the up-chirp and the down-chirp sections are  $B$ . The durations of the up-chirp and the down-chirp are  $T_1$  and  $T_2$ , respectively.  $\tau$  is the time delay between the transmitted signal and the received signal. Since the chirp rates of the up-chirp and the down-chirp sections are different, the de-chirped signals in the two sections show different frequencies ( $f_{up}$  and  $f_{dn}$ ), which is shown in Fig. 1(c) and (d).

Then, the de-chirped signal is sampled with a single-shot sub-Nyquist sampling process. Two aliased frequencies can be obtained, from which the values  $f_{up}$  and  $f_{dn}$  can be extracted as

$$\begin{cases} f_{up}^{i,k} = i \cdot f_{us} + k \cdot f_{a1} \\ f_{dn}^{j,l} = j \cdot f_{us} + l \cdot f_{a2} \end{cases} \quad (3)$$

where  $i$  and  $j$  are integers,  $k$  and  $l$  are  $\pm 1$ ,  $f_{a1}$  and  $f_{a2}$  are the aliased frequencies after sub-Nyquist sampling.

Fig. 2 shows the principle of the recovery algorithm in the modified Vernier sampling. According to (3), two sets of frequencies can be

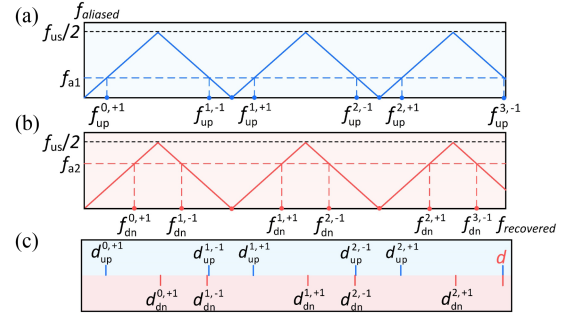


Fig. 2. Distance recovery from two aliased frequencies  $f_{a1}$  and  $f_{a2}$ . In (a) and (b), the horizontal and vertical axes are the recovered and aliased frequency, respectively. (c) Two sets of candidate distances and the recovered distance.

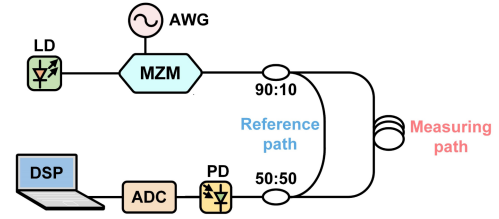


Fig. 3. Schematic diagram of the system. LD: Laser diode; AWG: Arbitrary waveform generator; MZM: Mach-Zehnder modulator; PD: Photodetector; ADC: Analog-to-digital converter; and DSP: Digital signal processing.

obtained from  $f_{a1}$  and  $f_{a2}$  in the up-chirp and the down-chirp sections, respectively. Then, two sets of distances are calculated according to (1), which are given by

$$\begin{cases} d_{up}^{i,k} = \frac{cT_1}{B} (i \cdot f_{us} + k \cdot f_{a1}) \\ d_{dn}^{j,l} = \frac{cT_2}{B} (j \cdot f_{us} + l \cdot f_{a2}) \end{cases} \quad (4)$$

where  $d_{up}^{i,k}$  and  $d_{dn}^{j,l}$  are the candidate distances. According to the principle of Vernier sampling, the first value that is present in both two sets is the recovered distance [labeled with  $d$  in red color in Fig. 3(c)], which can be expressed with a bijective function

$$d = (f_{a1}; i; k, f_{a2}; j; l) \quad (5)$$

It should be noted that the two aliased frequencies ( $f_{a1}$  and  $f_{a2}$ ) are simultaneously obtained in our proposed method due to the asymmetric waveforms. Therefore, it is feasible to determine the actual distance in a single-shot measurement. As a comparison, it always requires multiple parallel sampling processes in traditional Vernier sampling, which may change the system or add sampling devices.

However, in the proposed method, there is a minimum sampling rate, below which the distance recovery fails. In Vernier sampling, the least common multiple of the two sampling rates should be larger than the Nyquist sampling rate to ensure the distance recovery [22]. In our proposed method, the two aliased frequencies are simultaneously generated due to the two different chirp rates. As a result, the minimum sampling rate is limited by the ratio between the two chirp rates. The sub-Nyquist sampling ratio, which is defined as the ratio between the minimum rate and the Nyquist sampling rate, can be expressed as

$$\frac{f_{us}}{f_N} = \frac{1}{\text{LCM}(a, 1)} \quad (6)$$

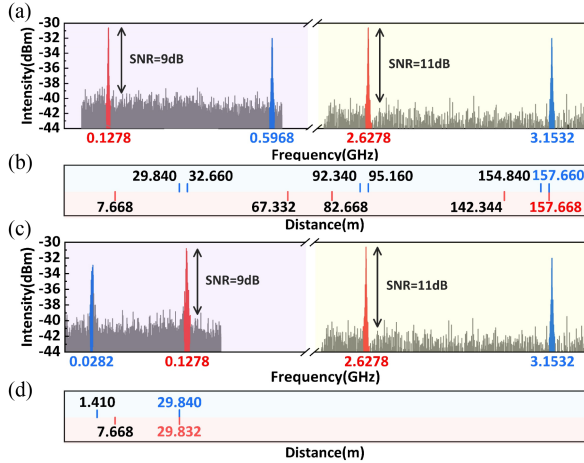


Fig. 4. Spectra of the de-chirped signals with the sampling rate of (a) 1.25 GHz and (c) 625 MHz. (b) and (d) show the distance recovery corresponding to (a) and (c). The ratio between the chirp rates is 1.2.

where  $f_N$  is the Nyquist sampling rate,  $a$  is the ratio of the two chirp rates, and  $\text{LCM}(x, y)$  is the least common multiple of  $x$  and  $y$ . It should be noted that the sub-Nyquist sampling ratio can be reconfigured readily by changing the modulation waveform. For example, if the durations of the up-chirp and the down-chirp sections are 1 and  $1.2 \mu\text{s}$ , the sub-Nyquist sampling ratio cannot be less than  $1/6$ . If the duration of the down-chirp sections is changed to  $1.1 \mu\text{s}$ , the minimum sub-Nyquist sampling ratio may be  $1/11$ .

### III. EXPERIMENT AND RESULTS

Fig. 3 shows the schematic diagram of the FMCW laser ranging system. A continuous-wave laser source (TeraXion PS-NLL) is used. A chirped RF signal is generated by an arbitrary waveform generator (AWG) and used to modulate the lightwave in a Mach-Zehnder modulator (MZM, Fujitsu FTM7938). Then, the modulated lightwave is divided by an optical coupler. One part is transmitted in the measuring path. The other part enters the reference path and beats with the measuring light in a photodetector (Finisar XPDV2120RA). An oscilloscope (OSC, Tektronix DSA72004B) is used to sample the beat signals at  $12.5 \text{ GSa/s}$ , which are then off-line sampled at different sub-Nyquist sampling rates. The bandwidth of the asymmetric chirped waveforms is 6 GHz.

Fig. 4 shows the measurement results of a 150-m fiber spool. The durations of the up-chirp and the down-chirp sections are 1 and  $1.2 \mu\text{s}$ . The blue and red lines represent the spectra in the up-chirp and down-chirp sections, respectively. The spectra of the fully sampled de-chirped signals are shown in the right section of Fig. 4(a), in which the de-chirped frequencies are 2.6278 and 3.1532 GHz, respectively. Then, the de-chirped signals are sampled at 1.25 GSa/s. The aliased spectra are shown in the left section of Fig. 4(a), in which the frequencies are 0.5968 and 0.1278 GHz, respectively. Moreover, the SNRs of the beat signals are reduced from around 11 dB to less than 9 dB after sub-Nyquist sampling.

According to (4), the distance can be recovered to be

$$\begin{cases} 157.6600 = 5 \times 10^{-8} \times (3 \times 1.25 - 0.5968) \times 10^9 \\ 157.6680 = 6 \times 10^{-8} \times (2 \times 1.25 + 0.1278) \times 10^9 \end{cases}$$

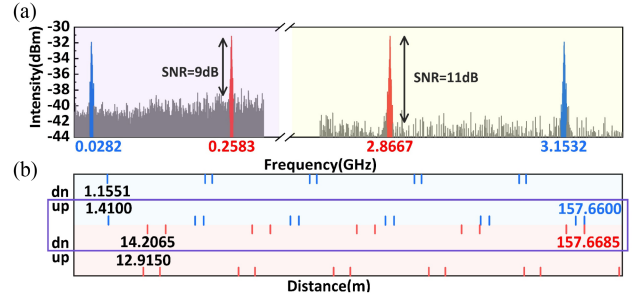


Fig. 5. (a) Spectra of the de-chirped signals at the sampling rate of 625 MHz. (b) Distance recovery corresponding to the spectra in (a). Ratio between the chirp rates is 1.1.

As a result, the recovered distance is  $157.6640 \pm 0.0040 \text{ m}$ . It should be noted that the recovered distance in the up-chirp and down-chirp sections is not equal. Therefore, the average of the two distances is used as the recovered distance. The difference between the recovered distances is used as the deviation of distance recovery. Meanwhile, the distance calculated from the full-sampled spectrum meets well with the recovered distance. The 1.25-GHz sampling rate is around  $1/5$  of the Nyquist sampling rate, which meets the requirement in (6). However, the sampling rate is difficult to be further reduced since it cannot be less than  $1/6$  of the Nyquist sampling rate. As shown in Fig. 4(c), when the sampling rate is 625 MHz, which is approximately  $1/10$  of the Nyquist sampling rate, an incorrect distance will be recovered at  $29.8360 \pm 0.0040 \text{ m}$  from the two aliased frequencies 0.1278 and 0.0282 GHz.

However, in the proposed method, the sub-Nyquist sampling ratio is reconfigurable by simply changing the ratio between the two chirp rates. Fig. 5 shows the measurement results, in which the duration of the down-chirp is changed to  $1.1 \mu\text{s}$ . As a result, the sampling rate can be reduced to less than  $1/10$  of the Nyquist sampling rate according to (6). In Fig. 5(a), the spectra obtained at the sampling rate of 625 MHz are shown in the left section. The two aliased frequencies are 0.0282 and 0.2583 GHz, respectively. The distance can be recovered as

$$\begin{cases} 157.6600 = 5 \times 10^{-8} \times (5 \times 0.625 + 0.0282) \times 10^9 \\ 157.6685 = 5.5 \times 10^{-8} \times (5 \times 0.625 - 0.2583) \times 10^9 \end{cases}$$

The recovered distance is  $157.6643 \pm 0.0043 \text{ m}$ , which is shown in the purple box in Fig. 5(b). As a comparison, the sampling rates are usually fixed so that the unaliased range of the distance cannot be reconfigured for traditional Vernier sampling.

The above distance recovery is based on *a priori* information. The mapping relationship between the aliased frequencies and the actual frequencies of the de-chirped signals is known. However, if both of the two aliased signals are simultaneously recorded in a measurement, an ambiguity may arise in the mapping relationship. For example, in Fig. 4(a) the aliased frequencies corresponding to 2.6278 GHz is lower than that corresponding to 3.1532 GHz. But, in Fig. 4(b), the aliased frequencies corresponding to 2.6278 GHz are the higher ones. In this case, four sets of distances have to be calculated according to (4). The recovery process is shown in Fig. 5(b), in which the ambiguity is solved and the measurement results are the same as the recovered distance based on the priori information.

In addition, the measurement errors of the proposed method are analyzed and shown in Fig. 6. As a comparison, the optical length of the measuring path is changed by inserting 0.51-m fiber patches.

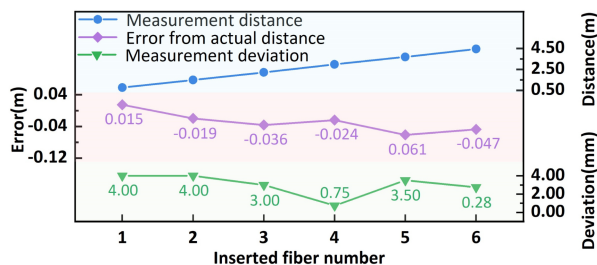


Fig. 6. Measurement errors of proposed FMCW ranging system. The ratio between the chirp rates is 1.1.

The de-chirped signal in 2 ms is recorded for spectrum analysis. The distance offset in Fig. 6 is 157.6643 m. The deviation of the distance recovered is shown as the green dotted line at the bottom of Fig. 6. As a comparison, the actual distance is measured using the homemade time delay measurement system [23], of which the accuracy is  $\pm 0.05$  ps ( $\pm 15$   $\mu$ m in optical length). The measurement error between the recovered distance and the actual distance is shown as the purple dotted line in the middle of Fig. 6. The measurement error is less than 6.1 cm, which is slightly larger than the theoretical resolution of the FMCW laser range.

Compared to traditional Vernier sampling, our method requires only a single-shot sampling, which reduces the number of hardware. The data processing of our proposed method only includes DFT and simple algorithms. Therefore, this work can reduce the sampling rates and data processing time without changing the system structure. Moreover, only the waveforms are changed in our method, which is easier to realize. The sub-Nyquist sampling ratio can be easily reconfigured by simply changing the waveforms. In addition, although it is hard to measure the velocity with this system, an FMCW laser ranging based on the optical carrier-suppressed dual-sideband (OC-DSB) modulation can adopt to measure the optical Doppler frequency [24]. The proposed sub-Nyquist sampling method can be used in the FMCW laser ranging system based on OC-DSB modulation so that both the distance and velocity can be simultaneously measured.

#### IV. CONCLUSION

We demonstrate an FMCW laser range with sub-Nyquist sampling rates. Using a modified Vernier sampling, the distance can be recovered from the two de-chirped frequencies in the asymmetric chirped waveforms with a single-shot sampling. By adjusting the ratio between the two chirp rates, the sub-Nyquist sampling ratio can be easily reconfigured. The length of fiber is measured using the proposed method with an accuracy of 6.1 cm, in which the sub-Nyquist sampling ratio can be adjusted from 1/5 to 1/10. The proposed method reduces the sampling rate and data volume of the FMCW laser ranging system, while no complex algorithm and additional sampling devices are required.

#### ACKNOWLEDGMENT

This work was supported in part by the National Natural Science Foundation of China (62171219) in part by the National Key R&D Program of China (2018YFB2201803), and in part by Jiangsu Natural Science Foundation (BK20190404).

#### REFERENCES

- [1] G. A. Howland, P. B. Dixon, and J. C. Howell, "Photon-counting compressive sensing laser radar for 3D imaging," *Appl. Opt.*, vol. 50, no. 31, pp. 5917–5920, 2011.
- [2] E. W. Mitchell et al., "Coherent laser ranging for precision imaging through flames," *Optica*, vol. 5, no. 8, pp. 988–995, 2018.
- [3] J. Cao et al., "Differential time domain method improves performance of pulsed laser ranging and three-dimensional imaging," *Appl. Opt.*, vol. 55, no. 2, pp. 360–367, 2016.
- [4] J. Kim, H. Cho, and S. Kim, "Positioning and driving control of fork-type automatic guided vehicle with laser navigation," *Int. J. Fuzzy Log. Intell. Syst.*, vol. 13, no. 4, pp. 307–314, 2013.
- [5] L. Yao, C. Qin, and Q. Chen, "Automatic road marking extraction and vectorization from vehicle-borne laser scanning data," *Remote Sens.*, vol. 13, no. 13, 2021, Art. no. 2612.
- [6] X. Mao, D. Inoue, S. Kato, and M. Kagami, "Amplitude-modulated laser radar for range and speed measurement in car applications," *IEEE Trans. Intell. Transp. Syst.*, vol. 13, no. 1, pp. 408–413, Mar. 2012.
- [7] A. Biasion, L. Bornaz, and F. Rinaudo, "Laser scanning applications on disaster management," in *Geo-Information for Disaster Management*, Berlin, Germany: Springer, 2005, pp. 19–33.
- [8] T. Oppikofer, M. Jaboyedoff, L. Blikra, M. -H. Derron, and R. Metzger, "Characterization and monitoring of the Aknes rockslide using terrestrial laser scanning," *Nat. Hazards Earth Syst. Sci.*, vol. 9, no. 3, pp. 1003–1019, 2009.
- [9] J. J. Degnan, "Satellite laser ranging: Current status and future prospects," *IEEE Trans. Geosci. Remote Sens.*, vol. GE-23, no. 4, pp. 398–413, Jul. 1985.
- [10] H. Ma, Y. Luo, Y. He, S. Pan, L. Ren, and J. Shang, "The short-range, high-accuracy compact pulsed laser ranging system," *Sensors*, vol. 22, no. 6, 2022, Art. no. 2146.
- [11] J. Riemensberger et al., "Massively parallel coherent laser ranging using a soliton microcomb," *Nature*, vol. 581, no. 7807, pp. 164–170, 2020.
- [12] M. C. Amann, T. M. Bosch, and M. Lescure, "Laser ranging: A critical review of unusual techniques for distance measurement," *Opt. Eng.*, vol. 40, pp. 10–19, 2001.
- [13] T. Hariyama, P. A. M. Sandborn, and M. Watanabe, "High-accuracy range-sensing system based on FMCW using low-cost VCSEL," *Opt. Express*, vol. 26, no. 7, pp. 9285–9297, 2018.
- [14] J. Ke et al., "Long distance high resolution FMCW laser ranging with phase noise compensation and 2D signal processing," *Appl. Opt.*, vol. 61, no. 12, pp. 3443–3454, 2022.
- [15] R. J. Marks, II: *Introduction to Shannon Sampling and Interpolation Theory*. Berlin, Germany: Springer, 1991.
- [16] J. Castorena and C. D. Creusere, "Sampling of time-resolved full-waveform LIDAR signals at sub-nyquist rates," *IEEE Trans. Geosci. Remote Sens.*, vol. 53, no. 7, pp. 3791–3802, Jul. 2015.
- [17] W. R. Babbitt, Z. W. Barber, and C. Renner, "Compressive laser ranging," *Opt. Lett.*, vol. 36, no. 24, pp. 4794–4796, 2011.
- [18] F. Li et al., "CS-ToF: High-resolution compressive time-of-flight imaging," *Opt. Express*, vol. 25, no. 25, pp. 31096–31110, 2017.
- [19] L. G. Abbas, "Vernier effect-based strain sensor with cascaded Fabry-Perot interferometers," *IEEE Sens. J.*, vol. 20, no. 16, pp. 9196–9201, Aug. 2020.
- [20] B. Hardy et al., "Vernier frequency sampling: A new tuning approach in spectroscopy—Application to multi-wavelength integrated path DIAL," *Appl. Phys. B*, vol. 107, no. 3, pp. 643–647, 2012.
- [21] S. Bak et al., "Optical vernier sampling using a dual-comb-swept laser to solve distance aliasing," *Photon. Res.*, vol. 9, no. 5, pp. 657–667, 2012.
- [22] X. G. Xia and K. Liu, "A generalized Chinese remainder theorem for residue sets with errors and its application in frequency determination from multiple sensors with low sampling rates," *IEEE Signal Process. Lett.*, vol. 12, no. 11, pp. 768–771, Nov. 2005.
- [23] S. Li, T. Qing, J. Fu, X. Wang, and S. Pan, "High-accuracy and fast measurement of optical transfer delay," *IEEE Trans. Instrum. Meas.*, vol. 70, 2021, Art. no. 8000204.
- [24] Z. Xu, L. Tang, H. Zhang, and S. Pan, "Simultaneous real-time ranging and velocimetry via a dual-sideband chirped lidar," *IEEE Photon. Technol. Lett.*, vol. 29, no. 24, pp. 2254–2257, Dec. 2017.